A Numerical Method of Determining the Rate of Evaporation of Small Water Drops Falling at Terminal Velocity in Air

S. E. WOO AND A. E. HAMIELEC

Dept. of Chemical Engineering, McMaster University, Hamilton, Ontario, Canada

(Manuscript received 23 April 1971, in revised form 9 July 1971)

ABSTRACT

Accurate, numerical solutions of the Navier-Strokes equations of motion and the equation of mass transfer have been obtained for the steady-state transfer of a chemically inert substance from the surface of a single rigid sphere moving at its terminal velocity in an unbounded fluid. Local Sherwood numbers have been calculated for spheres with Reynolds numbers in the range 0.05–300 and for a fluid with a Schmidt number of 0.71. The objective of this study was to model the effect of ventilation on the rate of evaporation of cloud drops falling at terminal velocity in air subsaturated with respect to water.

1. Introduction

Theoretical studies of the effect of forced convection on the mass or heat transport from a spherical body had, up to the present, only limited success, since for a complete description of the physical process, a simultaneous solution of the Navier-Stokes equations of motion and the continuity, or the energy, equation is required. Acrivos and Taylor (1962) and Rimmer (1968) used the singular perturbation technique to find the effect of forced convection on the heat transfer from an isothermal sphere. Froessling (1938), Zikmundová (1965), Baird and Hamielec (1962) and Garner and Keey (1958) used boundary layer theory to describe the effect of forced convection on the mass transport from a spherical body. While the former approach gives results which are applicable only to Reynolds numbers $N_{\mathrm{Re}}=2A\rho U_\infty/\mu\ll 1$ (LeClair *et al.*, 1970; Pruppacher *et al.*, 1970), where A is the radius of the spherical body, and U_∞, ρ and μ are, respectively, the free stream velocity, density, and dynamic viscosity of the fluid surrounding the body, the latter approach neglects transfer in the region of the eddy at the downstream end of the sphere and seems adequate for the forward flow region only with $N_{\mathrm{Re}}\gg 1$ and a suitably small diffusion boundary layer. In an intermediate region $1\lesssim N_{\mathrm{Re}}\lesssim 100$, Kinzer and Gunn (1951) and Abraham (1968) have developed a theory which describes mass and heat transfer by a model involving a transient transfer of packets of fresh environmental fluid to the surface of the spherical body. This theory remains tenuous because it is based on approximations regarding the relaxation time for mass and heat exchange between successive packets and ignores important characteristics of the flow field around a sphere.

The limitations of all three methods can be overcome by solving the Navier-Stokes equations of motion simultaneously with the continuity or energy equation by finite-difference techniques. The present paper presents such an approach for the determination of the effect of forced convection on the steady-state transfer of water vapor, assumed to be chemically inert and to diffuse from the surface of a moving, single, rigid water sphere into air considered as an unbounded, chemically inert fluid surrounding the sphere. In the present study it was assumed that air as well as water vapor follow the ideal gas laws. The assumption of modeling a water drop by a rigid water sphere is well justified for the present problem as long as $N_{\mathrm{Re}}\lesssim 300$, since it has been shown by LeClair *et al.* that for these Reynolds numbers the drag on a water drop is equivalent to the drag on a rigid sphere at the same Reynolds number. The steady-state approximation was justified by Beard (1970). The assumption of axisymmetric flow is justified up to $N_{\mathrm{Re}}\approx 300$, as discussed by Pruppacher *et al.* In the present study the effect of forced convection on mass transfer is expressed in the form of local and overall Sherwood numbers which were computed by a numerical method to be discussed below.

2. Theoretical background

From the literature it appears that there is some ambiguity in the definitions used for the Sherwood number N_{Sh}, especially since these are sometimes based on experimental or theoretical convenience. In the present study the Sherwood number shall be defined on the bases of mass fluxes. According to Bird *et al.* (1960), Fick's first law in a fixed reference frame can be written in terms of the mass flux for water vapor as

$$\rho_v \mathbf{u}_v = -\rho \mathfrak{D} \nabla\left(\frac{\rho_v}{\rho}\right) + \frac{\rho_v}{\rho}(\rho_v \mathbf{u}_v + \rho_d \mathbf{u}_d), \quad (1)$$

where $\rho_v \mathbf{u}_v$ is the mass flux of water vapor, $\rho_d \mathbf{u}_d$ the mass flux of dry air, ρ_v and ρ_d the densities of water vapor and dry air, $\mathbf{u}_v$ and $\mathbf{u}_d$ the velocities of the water vapor and dry air with respect to the stationary reference frame, $\mathfrak{D}$ the diffusivity of water vapor in air, ρ the total mass density of the moist air, and ρ_v/ρ the mass fraction of water vapor in moist air. At the surface of a spherical drop of radius A the radial component of the flux in spherical coordinates is

$$(\rho_v u_v)_A = -\rho_A \mathfrak{D}_A \left[\frac{\partial}{\partial r}\left(\frac{\rho_v}{\rho}\right)\right]_A \Big/ \left(1 - \frac{\rho_v}{\rho}\right)_A, \quad (2)$$

since $\rho_d \mathbf{u}_d = 0$ at $r = A$ from the dual boundary condition of no slip at the surface and no flow through the surface. By integrating the flux over the surface S, one obtains for the total evaporation rate

$$\int_S \rho_{vA} u_{vA} dS = -dm/dt = -\frac{\rho_A \mathfrak{D}_A}{[1-\rho_v/\rho]_A} \int_S \left[\frac{\partial(\rho_v/\rho)}{\partial r}\right]_A dS, \quad (3)$$

where dm/dt is the rate of change of mass of the drop. We may nondimensionalize (3) by writing

$$\frac{2A(dm/dt)}{4\pi A^2 \rho_A \mathfrak{D}_A \Delta(\rho_v/\rho)} = \frac{2A}{4\pi A^2 \Delta(\rho_v/\rho)(1-\rho_v/\rho)_A} \times \int_S \left(\frac{\partial(\rho_v/\rho)}{\partial r}\right)_A dS, \quad (4)$$

where $(\Delta\rho_v/\rho) = (\rho_{vA}/\rho_A) - (\rho_{v\infty}/\rho_\infty)$. A dimensionless parameter, the Sherwood number, may now be defined as

$$\bar{N}_{\mathrm{Sh}} \equiv \frac{(-dm/dt)(1-\rho_v/\rho)_A}{2\pi A \rho_A \mathfrak{D}_A \Delta(\rho_v/\rho)} = -\frac{1}{2\pi A \Delta(\rho_v/\rho)} \int_S \left(\frac{\partial \rho_v/\rho}{\partial r}\right)_A dS. \quad (5)$$

For the present study we assume that ρ and $\mathfrak{D}$ are constant. This approximation results in very little error for water drops evaporating in air, as discussed by Beard and Pruppacher (1971). Thus, with $\Delta\rho_v = \rho_{vA} - \rho_{v\infty}$, Eq. (5) becomes

$$\bar{N}_{\mathrm{Sh}} = \frac{(dm/dt)(1-\rho_v/\rho)_A}{2\pi A \mathfrak{D}_A \Delta\rho_v} = -\frac{1}{2\pi A \Delta\rho_v} \int_S \left(\frac{\partial \rho_v}{\partial r}\right)_A dS. \quad (6)$$

With this definition the right-hand side of (6), written in terms of the spherical coordinates r, θ, and φ, becomes

$$\bar{N}_{\mathrm{Sh}} = -\frac{1}{2\pi A \Delta\rho_v} \int_{\theta=0}^{\theta=\pi} \int_{\varphi=0}^{\varphi=2\pi} \left(\frac{\partial \rho_v}{\partial r}\right)_A r^2 \sin\theta d\theta d\varphi. \quad (7)$$

In axial symmetric flow $(\partial\rho_v/\partial r)_A$ is only a function of θ. Thus, at the sphere surface

$$\bar{N}_{\mathrm{Sh}} = -\frac{A}{\Delta\rho_v} \int_0^\pi \left(\frac{\partial \rho_v}{\partial r}\right)_A \sin\theta d\theta. \quad (8)$$

Introducing the dimensionless quantity

$$\eta = (\rho_v - \rho_{v\infty})/(\rho_{vA} - \rho_{v\infty}) = \frac{1}{\Delta\rho_v}(\rho_v - \rho_{v\infty})$$

and $r^* = r/A$, (8) may be rewritten as

$$\bar{N}_{\mathrm{Sh}} = -\int_0^\pi \left(\frac{\partial \eta}{\partial r^*}\right)_A \sin\theta d\theta, \quad (9)$$

where $-(\partial\eta/\partial r^*)_A$ has the meaning of a local, θ-dependent Sherwood number. Let us now consider two cases.

a. A stationary drop

For the special case of a stationary drop, $(\partial\rho_v/\partial r)_A$ in Eq. (6) and consequently $(\partial\eta/\partial r^*)_A$ in Eq. (9) are constant. Thus, (6) can be written as

$$\bar{N}_{\mathrm{Sh}} = -\frac{2A}{\Delta\rho_v}\left(\frac{d\rho_v}{dr}\right)_A. \quad (10)$$

The quantity $(d\rho_v/dr)_A$ may be evaluated from the continuity equation for water vapor which for steady state, $\partial\rho_v/\partial t = 0$, can be expressed as

$$\nabla \cdot (\rho_v \mathbf{u}_v) = 0. \quad (11)$$

In spherical coordinates the radial component of (11) is

$$\frac{d}{dr}(r^2 \rho_v u_{vr}) = 0, \quad (12)$$

from which it follows that

$$r^2 \rho_v u_{vr} = \text{constant}. \quad (13)$$

Introducing into this result Eq. (1) expressed for the stationary case, $\rho_d \mathbf{u}_d = 0$, and for ρ=constant and $\mathfrak{D}$=constant, we obtain

$$\frac{r^2}{(1-\rho_v/\rho)}\left(\frac{d\rho_v}{dr}\right) = \frac{A^2}{(1-\rho_v/\rho)_A}\left(\frac{d\rho_v}{dr}\right)_A = \text{constant}, \quad (14)$$

which, after integration, yields

$$\left(\frac{d\rho_v}{dr}\right)_A=\frac{\rho(1-\rho_v/\rho)_A}{A}\ln\frac{(1-\rho_v/\rho)_A}{(1-\rho_v/\rho)_\infty}. \quad (15)$$

Consequently, after substituting (15) into (10) we have

$$\bar{N}_{\mathrm{Sh}}=-\frac{2}{\Delta(\rho_v/\rho)}\left(1-\frac{\rho_v}{\rho}\right)_A\ln\frac{(1-\rho_v/\rho)_A}{(1-\rho_v/\rho)_\infty}. \quad (16)$$

Expanding the logarithm into a series, it can be shown for $(\rho_v/\rho)<1$ that

$$\bar{N}_{\mathrm{Sh}}\approx 2\left(1-\frac{\Delta\rho_v}{2\rho}\right)\approx 2[1-\mathrm{O}(10^{-3})] \quad (17)$$

for a typical situation in atmospheric clouds. Thus, under the assumptions made for a stationary drop, we find that $\frac{1}{2}N_{\mathrm{Sh}}=1.0$.

b. A falling drop

In the more general case of a spherical drop which is not stationary but moves at its terminal velocity through moist air, the quantity $(\partial\rho_v/\partial r)_A$ in (6), and consequently $(\partial\eta/\partial r^*)_A$ in (9), must be obtained from a simultaneous solution of the Navier-Stokes equations of motion and the continuity equation. For this purpose the continuity equation for water vapor, given by Eq. (11), was combined with the flux equation (1) to yield

$$\nabla\cdot(\rho_v\mathbf{u})=\rho_v\nabla\cdot\mathbf{u}+\mathbf{u}\cdot\nabla\rho_v=\nabla\cdot[\rho\mathfrak{D}\nabla(\rho_v/\rho)], \quad (18)$$

where $\mathbf{u}=(\rho_v\mathbf{u}_v+\rho_d\mathbf{u}_d)/(\rho_v+\rho_d)$. For steady-state conditions the Navier-Stokes equation of motion for moist air streaming past a drop may be written as

$$\rho(\mathbf{u}\cdot\nabla)\mathbf{u}=-\nabla p+\mu\nabla^2\mathbf{u}+\tfrac{1}{3}\mu\nabla(\nabla\cdot\mathbf{u}), \quad (19)$$

where p is the pressure, and μ the dynamic viscosity of moist air. The viscosity μ was assumed to be constant. This assumption is justifiable since, for water drops evaporating in air μ varies over the transfer path by at most a few percent. Assuming, as before, that the total density ρ is constant, the continuity equation for moist air and steady-state conditions, $\nabla\cdot(\rho\mathbf{u})=0$, becomes

$$\nabla\cdot\mathbf{u}=0. \quad (20)$$

Using (20) and ρ=constant and $\mathfrak{D}$=constant, (18) and (19) can be written as

$$\mathbf{u}\cdot\nabla\rho_v=\mathfrak{D}\nabla^2\rho_v, \quad (21)$$

$$\rho(\mathbf{u}\cdot\nabla)\mathbf{u}=-p\nabla+\mu\nabla^2\mathbf{u}. \quad (22)$$

The assumption of ρ=constant in (19) is justified by the results of Woo (1971) from which one can readily deduce that density gradient flow, or free convection, can be completely neglected for evaporating cloud and rain drops which fall at terminal velocity if one considers the Schmidt number, given by $\mu/(\rho\mathfrak{D})$, the Reynolds numbers, and corresponding drop sizes involved.

An inspection of Eqs. (21) and (22) shows that, with the assumptions made, the Navier-Stokes equation of motion is independent of the mass transport equation for water vapor except for its coupling through the equation of state and the boundary conditions, whereas the mass transport equation is linked directly to the Navier-Stokes equation through the velocity field.

Introducing the dimensionless quantities

$$\left.\begin{array}{c}\overset{*}{\mathbf{u}}=\mathbf{u}/U_\infty;\quad \overset{*}{r}=r/A;\quad \overset{*}{p}=p/\tfrac{1}{2}\rho U_\infty^2\\ \overset{*}{\nabla}=A\nabla;\quad \eta=\dfrac{\rho_v-\rho_{v\infty}}{\rho_{vA}-\rho_{v\infty}}\end{array}\right\}, \quad (23)$$

and the Péclet number, $N_{\mathrm{Pe}}=N_{\mathrm{Sc}}N_{\mathrm{Re}}$, Eqs. (21) and (22) can be written in dimensionless form as

$$\frac{N_{\mathrm{Re}}}{2}(\overset{*}{\mathbf{u}}\cdot\overset{*}{\nabla})\overset{*}{\mathbf{u}}=-\frac{N_{\mathrm{Re}}}{4}\overset{*}{\nabla}\overset{*}{p}+\overset{*}{\nabla}{}^2\overset{*}{\mathbf{u}}, \quad (24)$$

$$\frac{N_{\mathrm{Pe}}}{2}\overset{*}{\mathbf{u}}\cdot\overset{*}{\nabla}\eta=\overset{*}{\nabla}{}^2\eta. \quad (25)$$

Because of its axial symmetry the flow may be described in terms of a streamfunction ψ which allows (24) to be expressed as a single scalar equation. Using spherical conditions, the dimensionless streamfunction, $\psi^*=\psi/U_\infty A^2$, and the nondimensionalized vorticity, $\xi^*=\xi A/U_\infty$, (24) can be written, after dropping the superscript, as

$$\frac{N_{\mathrm{Re}}}{2}\left[\frac{\partial\psi}{\partial r}\frac{\partial}{\partial\theta}\left(\frac{\xi}{r\sin\theta}\right)-\frac{\partial\psi}{\partial\theta}\frac{\partial}{\partial r}\left(\frac{\xi}{r\sin\theta}\right)\right]\sin\theta=E^2(\xi r\sin\theta), \quad (26)$$

with

$$E^2\psi=\xi r\sin\theta, \quad (27)$$

where

$$E^2=\frac{\partial^2}{\partial r^2}+\frac{\sin\theta}{r^2}\frac{\partial}{\partial\theta}\left(\frac{1}{\sin\theta}\frac{\partial}{\partial\theta}\right),$$

and where θ is the angular spherical coordinate measured from the foreword stagnation point on the sphere. The following boundary conditions apply to the problem: 1) along the axis of symmetry $\theta=0,\ \pi,\ \psi=0,\ \xi=0$; 2) on the sphere surface $r=1,\ \psi=0,\ \xi=E^2\psi/\sin\theta$; and 3) on the boundary remote from the surface of the sphere and concentric with the sphere $r=r_\infty,\ \psi=\frac{1}{2}r_\infty^2\times\sin^2\theta$.

Eqs. (26) and (27) were solved numerically by LeClair *et al.* The flow fields obtained by these authors were used in the present study to solve the continuity equation (25), which in spherical coordinates for axisymmetric flow can be written as

$$\frac{N_{\mathrm{Pe}}}{2}\left[\frac{\partial\psi}{\partial r}\frac{\partial\eta}{\partial\theta}-\frac{\partial\psi}{\partial\theta}\frac{\partial\eta}{\partial r}\right]=\sin\theta\left[r^2\frac{\partial^2\eta}{\partial r^2}+2r\frac{\partial\eta}{\partial r}+\cot\theta\frac{\partial\eta}{\partial\theta}+\frac{\partial^2\eta}{\partial\theta^2}\right]. \quad (28)$$

A significant savings of computation time was achieved by making the transformation $r^*=e^z$; in this case (28) becomes

$$\frac{N_{\mathrm{Pe}}}{2}\left[\frac{\partial\psi}{\partial z}\frac{\partial\eta}{\partial\theta}-\frac{\partial\psi}{\partial\theta}\frac{\partial\eta}{\partial z}\right]=\exp(z)\sin\theta\left[\frac{\partial^2\eta}{\partial z^2}+\frac{\partial\eta}{\partial z}+\cot\theta\frac{\partial\eta}{\partial\theta}+\frac{\partial^2\eta}{\partial\theta^2}\right]. \quad (29)$$

Eq. (29) was solved for the boundary conditions: 1) $\eta=1$ at $z=0$; 2) $\eta=0$ at $z=\infty$; and 3) $\partial\eta/\partial\theta=0$ at $\theta=0, \pi$. Overall Sherwood numbers were then computed from (9) which, after introducing $r^*=e^z$, can be written as

$$\bar{N}_{\mathrm{Sh}}=\int_0^\pi N_{\mathrm{Sh}}(\theta)\sin\theta d\theta. \quad (30)$$

Local Sherwood numbers were found from

$$N_{\mathrm{Sh}}(\theta)=-\left[\frac{\partial\eta(\theta)}{\partial z}\right]_{z=0}. \quad (31)$$

3. Numerical analysis

Eq. (29) was discretized using formulas accurate to second order according to the mesh system given in Fig. 1. The discrete equation is

$$\begin{aligned}\eta(I,J)=\Bigg\{&\eta(I,J+1)\left[\frac{1}{H^2}+\frac{1}{2H}+\frac{N_{\mathrm{Pe}}}{8HGe^z\sin\theta}(\psi(I+1,J)-\psi(I-1,J))\right]\\&+\eta(I,J-1)\left[\frac{1}{H^2}-\frac{1}{2H}-\frac{N_{\mathrm{Pe}}}{8HGe^z\sin\theta}(\psi(I+1,J)-\psi(I-1,J))\right]\\&+\eta(I+1,J)\left[\frac{1}{G^2}+\frac{\cot\theta}{2G}-\frac{N_{\mathrm{Pe}}}{8GHe^z\sin\theta}(\psi(I,J+1)-\psi(I,J-1))\right]\\&+\eta(I-1,J)\left[\frac{1}{G^2}-\frac{\cot\theta}{2G}+\frac{N_{\mathrm{Pe}}}{8GHe^z\sin\theta}(\psi(I,J+1)-\psi(I,J-1))\right]\Bigg\}\frac{H^2G^2}{2(H^2+G^2)}, \quad (32)\end{aligned}$$

where H is the lattice spacing in radial direction, G the lattice spacing in angular direction, and N the

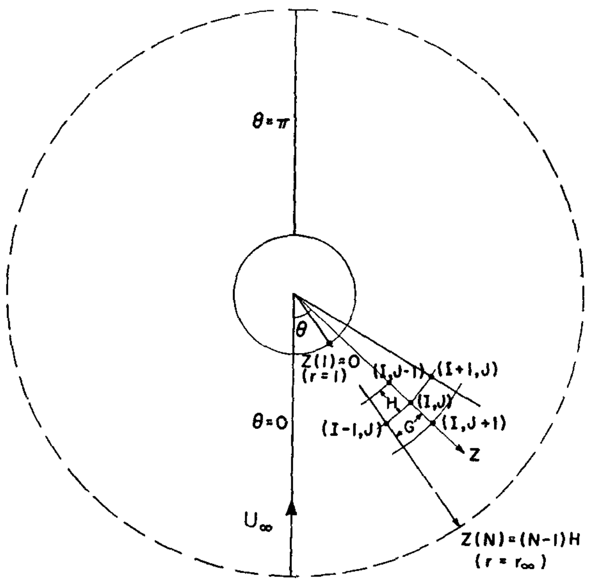

FIG. 1. Spherical mesh system employed in present numerical method.

TABLE 1. Step size and wall effect errors in overall Sherwood numbers ($N_{\mathrm{Sc}}=0.71$) calculated by present numerical method.

Step size error ($N_{\mathrm{Re}}=300$)		
H	G	$\bar{N}_{\mathrm{Sh}}$
0.05	6°	11.60
0.025	3°	10.95

Wall effect error ($N_{\mathrm{Re}}=0.2$)	
r_∞	$\bar{N}_{\mathrm{Sh}}$
49	2.0638
134	2.0582
365	2.0582

TABLE 2. Parameters used for the present numerical solution of the mass transfer equation ($N_{\mathrm{Sc}}=0.7$).

N_{Re}	N	H	G	r_∞
0.05–1	50	0.1	6°	134
2	40	0.1	6°	49.4
3–5	70	0.05	6°	31.5
10–57	35	0.05	6°	5.47
100	65	0.025	3°	4.95
200,300	70	0.025	3°	5.61

TABLE 3. Local Sherwood numbers calculated by present numerical method as a function of Reynolds number and angle from frontal stagnation point ($N_{Sc}=0.71$).

N_{Re}	Angle from frontal stagnation point (deg) 0	12	24	36	48	60	72	84	96	108	120	132	144	156	168	180
300	21.34	21.09	20.50	19.51	18.13	16.35	14.16	11.57	8.74	6.02	3.95	3.38	4.51	6.95	9.03	10.15
200	17.38	17.18	16.72	15.96	14.90	13.53	11.86	9.92	7.81	5.73	3.99	3.02	3.43	5.04	6.60	7.25
100	12.43	12.29	11.98	11.48	10.78	9.89	8.82	7.60	6.29	5.00	3.84	2.97	2.55	2.64	2.97	3.18
57	9.75	9.64	9.40	9.01	8.49	7.83	7.06	6.21	5.31	4.42	3.61	2.94	2.50	2.29	2.25	2.27
30	7.26	7.18	7.02	6.77	6.42	5.98	5.48	4.92	4.34	3.76	3.22	2.77	2.43	2.12	2.11	2.10
10	4.64	4.59	4.52	4.39	4.22	4.01	3.76	3.50	3.22	2.95	2.69	2.46	2.28	2.14	2.06	2.05
5	3.65	3.61	3.56	3.48	3.38	3.25	3.10	2.94	2.77	2.60	2.45	2.31	2.19	2.11	2.06	2.06
3	3.15	3.11	3.08	3.02	2.95	2.86	2.76	2.65	2.54	2.42	2.32	2.22	2.15	2.09	2.05	2.05
2	2.83	2.81	2.79	2.75	2.70	2.63	2.56	2.48	2.39	2.31	2.24	2.17	2.11	2.07	2.04	2.04
1	2.48	2.46	2.45	2.43	2.39	2.36	2.32	2.27	2.23	2.18	2.14	2.10	2.07	2.05	2.04	2.04
0.75	2.38	2.36	2.35	2.33	2.31	2.28	2.25	2.21	2.18	2.14	2.11	2.08	2.06	2.04	2.03	2.03
0.5	2.27	2.26	2.25	2.23	2.22	2.20	2.17	2.15	2.13	2.10	2.09	2.06	2.04	2.03	2.02	2.02
0.2	2.12	2.11	2.11	2.10	2.09	2.08	2.08	2.06	2.06	2.04	2.03	2.03	2.02	2.01	2.01	2.01

number of mesh points in radial direction. In the numerical solution, the boundary condition at $z=\infty$ is closely simulated by satisfying the condition at a distant but finite distance from the sphere surface, *viz.*,

$$z=(N-1)H, \quad \eta=0. \tag{33}$$

Suitable values of N, H and G were found by trial and error. The wall effect error is greatest at low Péclet numbers. In order to estimate this error, a very thorough investigation was made of the effect of N on the calculated average Sherwood number for the case $N_{Re}=0.2$ and $N_{Sc}=0.71$. The step size error is greatest at high Péclet numbers. In order to estimate this error the effect of a change in H and G on the average Sherwood number was investigated for the case $N_{Re}=300$ and $N_{Sc}=0.71$. The results of these investigations are given in Table 1. Based on an examination of the above errors, the parameters in Table 2 were chosen for the solution of (32), which was solved on a CDC 6400 computer using an iterative method fully described by Woo (1971). The solutions were assumed to have converged when the normalized error per iteration in η at all mesh points was less than 10^{-4}. This should give an error in the average Sherwood number for all the Reynolds numbers investigated of less than 0.1%.

4. Results and discussion

The results of our analysis are summarized in Tables 3–5 and Figs. 2–4. In Table 3 local Sherwood numbers have been tabulated for $0.2 \leqslant N_{Re} \leqslant 300$ and for $N_{Sc}=0.71$ which is appropriate for water vapor diffusing through air. In Fig. 2 the variation of the local Sherwood number with θ is given for $N_{Sc}=0.71$ and for $57 \leqslant N_{Re} \leqslant 300$, indicating the effect of flow separation on the mass transport. In Fig. 3 the flow pattern is exhibited which caused the distribution of the local Sherwood number at $N_{Re}=200$. At this relatively high Reynolds number the fluid velocity along $\theta=\pi$ is directed toward the rear stagnation point and is of sufficient magnitude to raise the local Sherwood number appreciably above the limiting value $N_{Sh}=2$ for a stationary sphere. For $57 \leqslant N_{Re} \leqslant 300$ the minimum local Sherwood number occurs at $\theta<180°$. A comparison between the angle of flow separation θ_S and the angle θ_M of the minimum local Sherwood number (both θ_S and θ_M are measured from the rear stagnation point) is made in Table 4 for $N_{Sc}=0.5$, 0.71, 1.0. This comparison is graphically displayed in Fig. 4. Table 4 and Fig. 4 show that at $N_{Re}<40$ the minimum local Sherwood number is always found at the rear stagnation point. In this Reynolds number range, the use of mass transfer measurements to estimate the flow separation angle θ_S would lead to ap-

TABLE 4. Comparison between the flow separation angle and angles for minimum local Sherwood number as a function of Reynolds number and Schmidt number.

N_{Re}	θ_S	θ_M (for N_{Sc} values of) 0.5	0.71	1.0
300	68.4	48	51	53.4
200	63.3	42	45	47.4
100	52.8	30	33	36
57	43.5	6	12	18
30	27.4	0	0	0
20	0	0	0	0

TABLE 5. Variation with Reynolds number of the overall Sherwood number calculated by present numerical method ($N_{Sc}=0.71$).

N_{Re}	$\bar{N}_{Sh}$
0.05	2.016
0.10	2.028
0.20	2.058
0.50	2.136
0.75	2.194
1.0	2.246
2.0	2.430
3.0	2.588
5.0	2.843
10	3.34
30	4.61
57	5.75
100	6.98
200	9.22
300	10.95

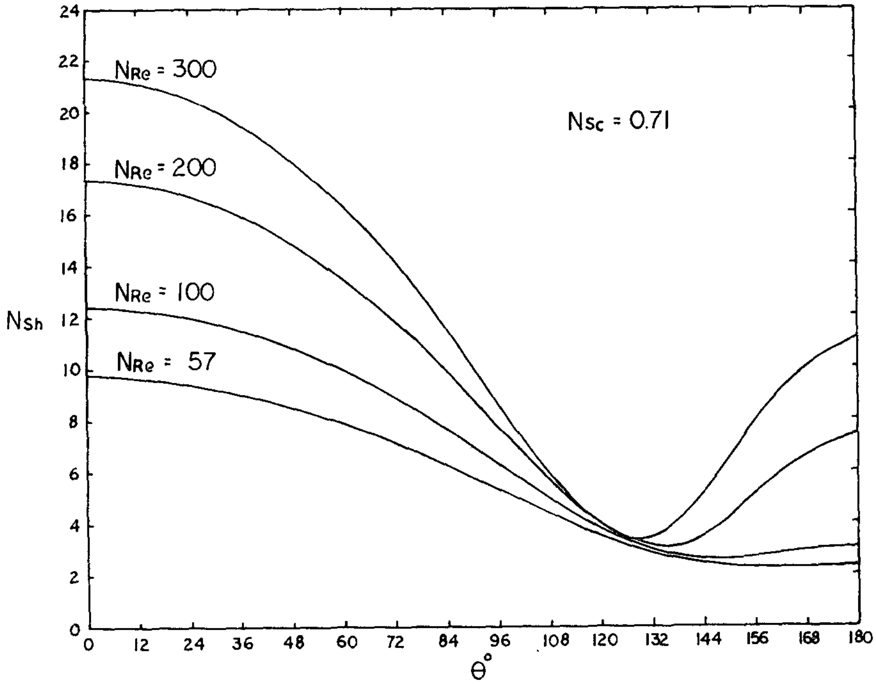

Fig. 2. Local Sherwood numbers calculated by present numerical method for $N_{Sc}=0.71$ and $57 \leqslant N_{Re} \leqslant 300$.

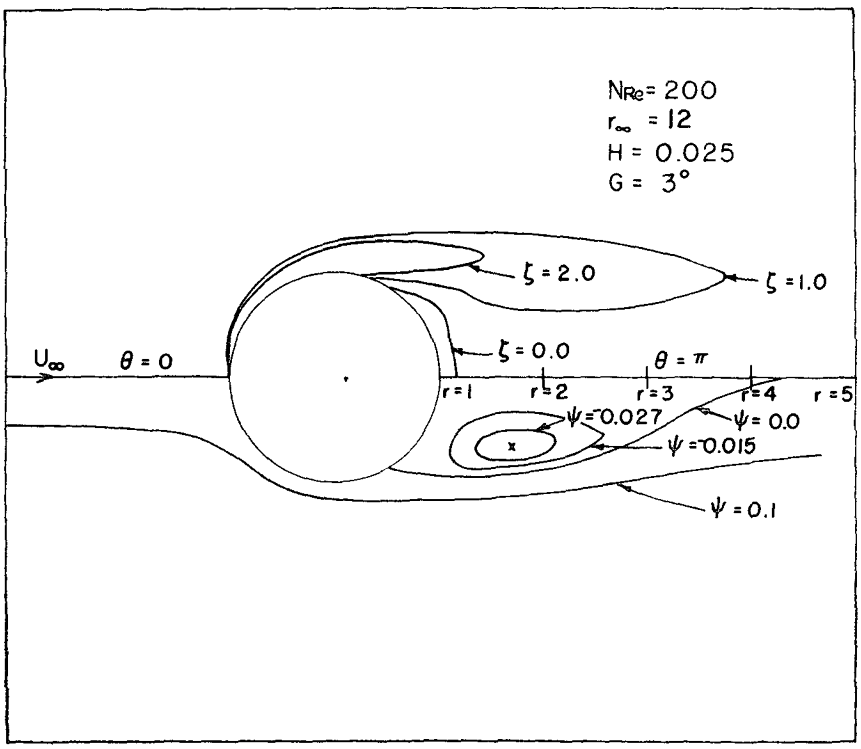

Fig. 3. Lines of constant vorticity and streamlines showing local flow behavior calculated by present numerical method for $N_{Re}=200$.

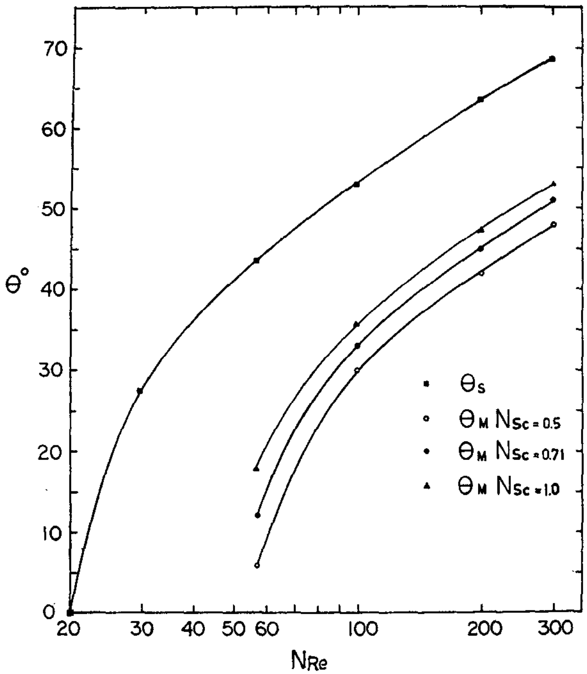

FIG. 4. Flow separation angles and angles at point of minimum local Sherwood number calculated by present numerical method for $20 \leqslant N_{Re} \leqslant 300$ and $0.5 \leqslant N_{Sc} \leqslant 1.0$.

preciable errors with θ_M always being significantly smaller than θ_S at $N_{Sc}=0.71$. Even though the difference between θ_S and θ_M becomes smaller with increasing Schmidt numbers, there remains a significant discrepancy at $N_{Re}=300$. In Table 5 overall Sherwood numbers are tabulated for $0.05 \leqslant N_{Re} \leqslant 300$. A comparison between these values and recent experimental data is made by Beard and Pruppacher (1971).

Acknowledgments. The authors would like to express their gratitude to the National Research Council of Canada for supporting the present research. They also wish to acknowledge the fruitful discussions with Prof. Hans R. Pruppacher, Dept. of Meteorology, University of California, Los Angeles, during the preparation of this manuscript.

REFERENCES

Abraham, F., 1968: A physical interpretation of the structure of the ventilation coefficients for freely falling water drops. *J. Atmos. Sci.*, **25**, 76–81.

Acrivos, A., and T. D. Taylor, 1962: Heat and mass transfer from single spheres in Stokes flow. *Phys. Fluids*, **5**, 387–394.

Baird, M. H. I., and A. E. Hamielec, 1962: Forced convection transfer around spheres at intermediate Reynolds numbers. *Can. J. Chem. Eng.*, **40**, 119–121.

Beard, K. V., 1970: A wind tunnel investigation of the terminal fall velocities, collection kernels and ventilation coefficients of water drops freely falling in air. Ph.D. thesis, Dept. of Meteorology, University of California, Los Angeles.

——, and H. R. Pruppacher, 1971: A wind tunnel investigation of the rate of evaporation of small water drops falling at terminal velocity in air. *J. Atmos. Sci.*, **28**, 1445–1464.

Bird, R. B., W. E. Stewart and E. N. Lightfoot, 1960: *Transport Phenomena*. New York, Wiley 780 pp.

Froessling, N., 1938: Ueber die Verdunstung fallender Tropfen. *Beitr. Geophys.*, **52**, 170–216.

Garner, F. H., and R. B. Keey, 1958: Mass transfer from single, solid spheres. *Chem. Eng. Sci.*, **9**, 119–129.

Kinzer, G. D., and R. Gunn, 1951: The evaporation, temperature and thermal relaxation time of freely falling water drops. *J. Meteor.*, **8**, 71–83.

LeClair, B. P., A. E. Hamielec and H. R. Pruppacher, 1970: A numerical study of the drag on a sphere at low and intermediate Reynolds numbers. *J. Atmos. Sci.*, **27**, 308–315.

Pruppacher, H. R., B. P. LeClair and A. E. Hamielec, 1970: Some relations between drag and flow pattern of viscous flow past a sphere and a cylinder at low and intermediate Reynolds numbers. *J. Fluid Mech.*, **44**, 781–790.

Rimmer, P. L., 1968: Heat transfer from a sphere in a stream with small Reynolds number. *J. Fluid Mech.*, **32**, 1–7.

Woo, S. W., 1971: Simultaneous free and forced convection around submerged cylinders and spheres. Ph.D. thesis, Dept. of Chemical Engineering, McMaster University, Hamilton, Canada.

Zikmundová, J., 1965: On the evaporation of water drops. *Proc. Intern. Conf. Cloud Physics*, Toronto, Canada, 364–368.